

OPEN ACCESS

Experimental and numerical investigation on damping properties and energy dissipation mechanisms of magnetosensitive rubber

To cite this article: W Li *et al* 2013 *J. Phys.: Conf. Ser.* **412** 012030

View the [article online](#) for updates and enhancements.

You may also like

- [Energy dissipation characteristics of magnetosensitive elastomer under impact loading](#)
D Leng, L Sun, J Sun *et al.*
- [The Magnetic Isotopes Effect of Magnesium ²⁵Mg on the Physiological Properties of Bacteria *E. coli*](#)
U G Letuta and T A Tikhonova
- [Highly sensitive surface acoustic wave magnetic field sensor based on the loss mechanism](#)
Yutong Wu, Baile Cui, Yana Jia *et al.*



ECS
The
Electrochemical
Society
Advancing solid state &
electrochemical science & technology

DISCOVER
how sustainability
intersects with
electrochemistry & solid
state science research

Experimental and numerical investigation on damping properties and energy dissipation mechanisms of magnetosensitive rubber

W Li, L Sun¹, J Sun, W Chen, F Ma and D Leng

School of Transportation Science and Engineering, Beihang University,
Beijing 100191, China

E-mail: lysunluck@gmail.com

Abstract: This study presents both numerical and experimental investigation on damping properties and energy dissipation mechanisms of magnetosensitive rubber (MSR). Representative volume element (RVE) including particles and matrix was built and periodic boundary condition (PBC) was applied. Various sinusoidal loads, with different frequencies, were applied to RVE under external magnetic field. Considering interaction and complex mechanisms in multi-physics field, finite element method (FEM) based on magneto-mechanical coupling algorithm was adopted. MSR samples were fabricated by aligning iron particles with millimeter level diameter in silicone rubber matrix. The correctness of the numerical method was verified by comparing the results of simulation and quasi-static load test. Dynamic experimental measurement was conducted in material test system. The results demonstrate that the damping properties of MSR are influenced by magnetic induction density and frequency of sinusoidal load. Energy dissipation mechanisms of MSR were explored.

1. Introduction

Magnetorheological elastomers (MREs) are a class of smart materials whose mechanical properties can be controlled by external magnetic field [1]. Besides adjustable elastic properties, it is experimentally demonstrated that MREs also have controllable damping properties [2-4] which possibly can be applied in vibration environment as damper materials. Similar to elastic properties, MREs' damping properties are also probably influenced by both internal factors (shape, size and volume fraction of particle, etc.) and external factors (direction, amplitude, frequency of structural load and magnetic field, etc).

However, the previous experimental and numerical researches mainly focused on studying the relationship between mechanical characteristics of MREs and influencing factors [5-10]. For MREs, complete explanation in terms of the distribution of stress field and magnetic field has not been introduced in detail yet. In order to utilize MREs as damper materials effectively, it is necessary to explore the damping properties and understand the energy dissipation mechanisms by studying their stress field and magnetic field

This research introduced MSR whose structure is very similar to MRE and studied the mechanical characteristics of MSR numerically and experimentally.

¹ Corresponding author.

2. Experiment

2.1. Fabrication of MSR

Traditionally, MREs are fabricated of carbonyl iron powder with micron level particle size, silicone rubber and additives. Because the dimensions of particles and the distance between adjacent particles are rather small, the microstructure of MREs needs to be observed by scanning electron microscopy (SEM). It is difficult to install test probes in the small gap between the magnetized particles to measure magnetic field without destroying the integrity of matrix structure and the distribution of magnetic field. It is also difficult to get stress/strain field of MREs. Hence, iron particles (Puning Iron Particle Factory, China) with millimeter level diameter and transparent silicone rubber (Kenseer Polymer Technology Co., Ltd. China, Model: SE901A and SE901B) are used. This new type of MRE is named as MSR. In the future work, small Hall probes can be installed in MSR. Moreover, photoelastic technology may be used to measure stress field of it. Although there are some differences between MSR and MRE, it will be very helpful to understand mechanical characteristics of MRE by analogical and comparative method.

Particles are aligned in two ways, uniform or chain-like, shown as Figure 1(a) and (b), respectively. Because the elongation is below 10%, the particle arrangement can keep initial configurations in experimental set up well. The diameter of iron particles is 8 mm. The volume fraction of iron particles is 27% which is optimum predicted by Davis [11]. The sizes of samples are about 32mm×32mm×32mm (uniform particles arrangement) and 28mm×35mm×35mm (chain-like particles arrangement), respectively (Because manufacturing error and measurement error, the volume fraction of iron particles is not absolutely 27%). Each sample contains 3×3×3, a total of 27 iron particles. The ratio of distance (W) between adjacent particles in the chain and particle diameter (D) is 0.05, shown as figure 2. The mixing ratio of SE901A and SE901B is 1:1. The mixture is placed in vacuum tank for twenty minutes to remove all air bubbles. During pre-configuration stage, the samples are heated to about 100°C for total of 1 h in a specific mold covered by plastic sheeting, shown as figure 3.

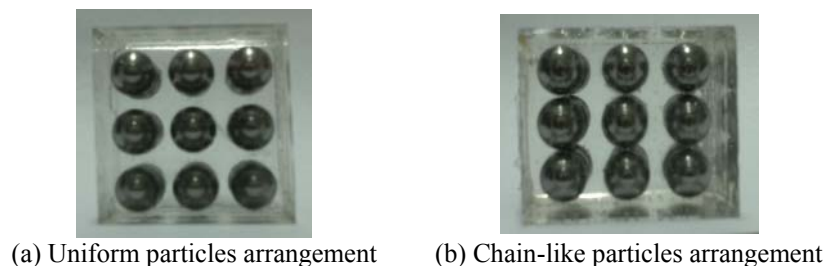


Figure 1. MSR samples.

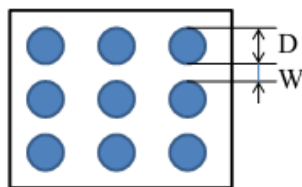


Figure 2. Schematic of MSR.

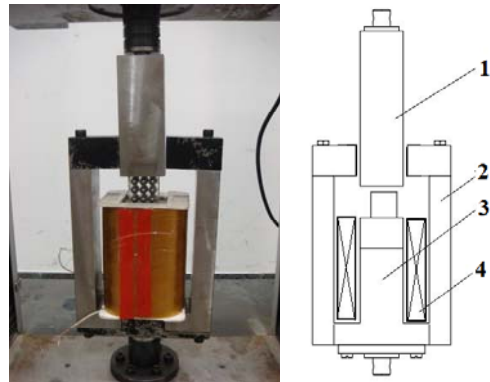


Figure 3. Iron mold.

2.2. Experimental setup

A set of iron fixture including connector base and core is used to install sample and connect to loading device, shown as Figure 4. The magnetic field ranging from 0 mT to 400 mT is generated by the built-

in electromagnet coil. Teslameter (Weite Magnetolectric Engineering Corp, China, Model: WT-10A,) is used to measure the magnetic induction density. MTS-880 material test system is used for both static and dynamic experiments to measure tensile modulus and damping capacity of MRE.



1-connector 2-base 3-core 4-electromagnet coil

Figure 4. Experimental setup.

3. Numerical investigation

3.1. Representative volume element

Besides using iron particles with millimeter level diameter and transparent silicone rubber, finite element techniques can also help to analyze the distribution of magnetic field and stress field.

Each MSR sample contains twenty-seven iron particles. If all particles are included in the 3-D finite element model, it will need so much computational time. Therefore, the characteristics of MSR can be obtained by RVE. For composite materials, the mechanical characteristics of RVE in micro-scale can represent the material properties of structure in macro-scale well. Three typical RVE modes are presented, shown as Figure 5. Type 1 shows that a spherical particle is surrounded by matrix. Type 2 shows that two hemispherical particles embed in the upper side and lower side of matrix. Type 3 shows that eight 1/8 spherical particles distribute in the corners of the cube. Each type of RVE is $2P_x$ width, $2P_y$ length and $2P_z$ height, shown as Figure 6. The chain is along z-axis direction.

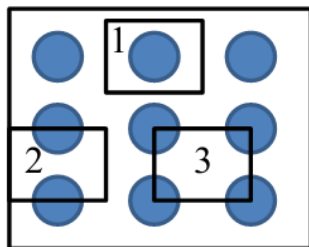


Figure 5. Three typical RVE modes.

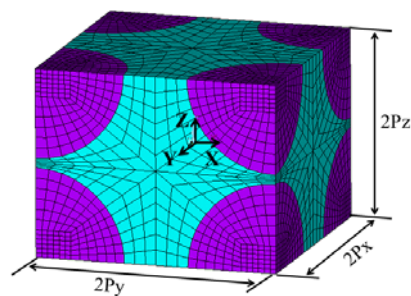


Figure 6 Size of RVE.

When applying magnetic field along the chain, the magnetic force between the adjacent particles within chain and that in different chain both will influence characteristics of RVE, shown as Figure 7. So, type 3 is chosen to analyze.

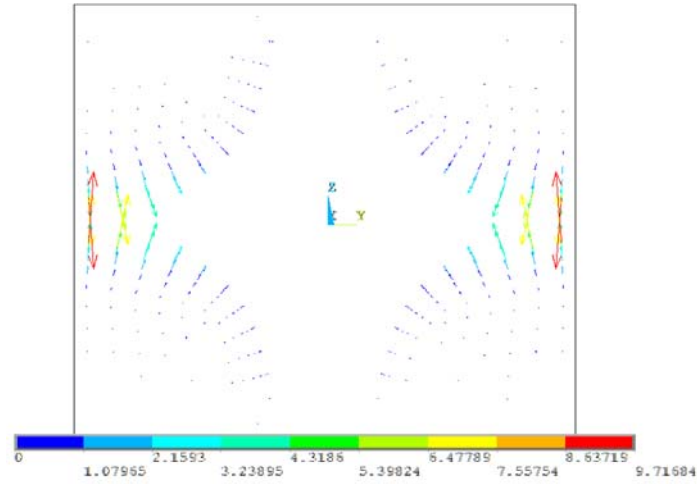


Figure 7. Magnetic force between adjacent particles under 1 T magnetic field.

3.2. Periodic boundary condition

When applying constant or sinusoidal loads along chain, the PBC of RVE is described by equation (1)-(3):

Compatibility equations between left surface and right surface of RVE are:

$$\begin{cases} u(P_x, y, z) - u(-P_x, y, z) = 2\varepsilon_x P_x \\ v(P_x, y, z) - v(-P_x, y, z) = 0 \\ w(P_x, y, z) - w(-P_x, y, z) = 0 \end{cases} \quad (1)$$

Compatibility equations between front surface and rear surface of RVE are:

$$\begin{cases} u(x, P_y, z) - u(x, -P_y, z) = 0 \\ v(x, P_y, z) - v(x, -P_y, z) = 2\varepsilon_y P_y \\ w(x, P_y, z) - w(x, -P_y, z) = 0 \end{cases} \quad (2)$$

Compatibility equations between top surface and bottom surface of RVE are:

$$\begin{cases} u(x, y, P_z) - u(x, y, -P_z) = 0 \\ v(x, y, P_z) - v(x, y, -P_z) = 0 \\ w(x, y, P_z) - w(x, y, -P_z) = \delta_t = A \sin(2\pi ft) \end{cases} \quad (3)$$

Where, u , v and w denotes the displacement along x-axis, y-axis and z-axis, respectively.

ε_x and ε_y represents strain in x-direction and y-direction, respectively.

δ_t is tension-compression loads of z-direction and f is frequency, respectively.

3.3. Finite element method

Sequential magneto-mechanical coupling algorithm which can solve specific static and dynamic problems is written in ANSYS APDL language, the flowchart is shown in Figure 8.

Either magnetic field or mechanical field can be calculated first, and then the numerical information of magnetic field or mechanical field will be transferred to another field. By several calculation cycles, the stress/strain field and the magnetic field will be constant which indicates that RVE is in equilibrium state.

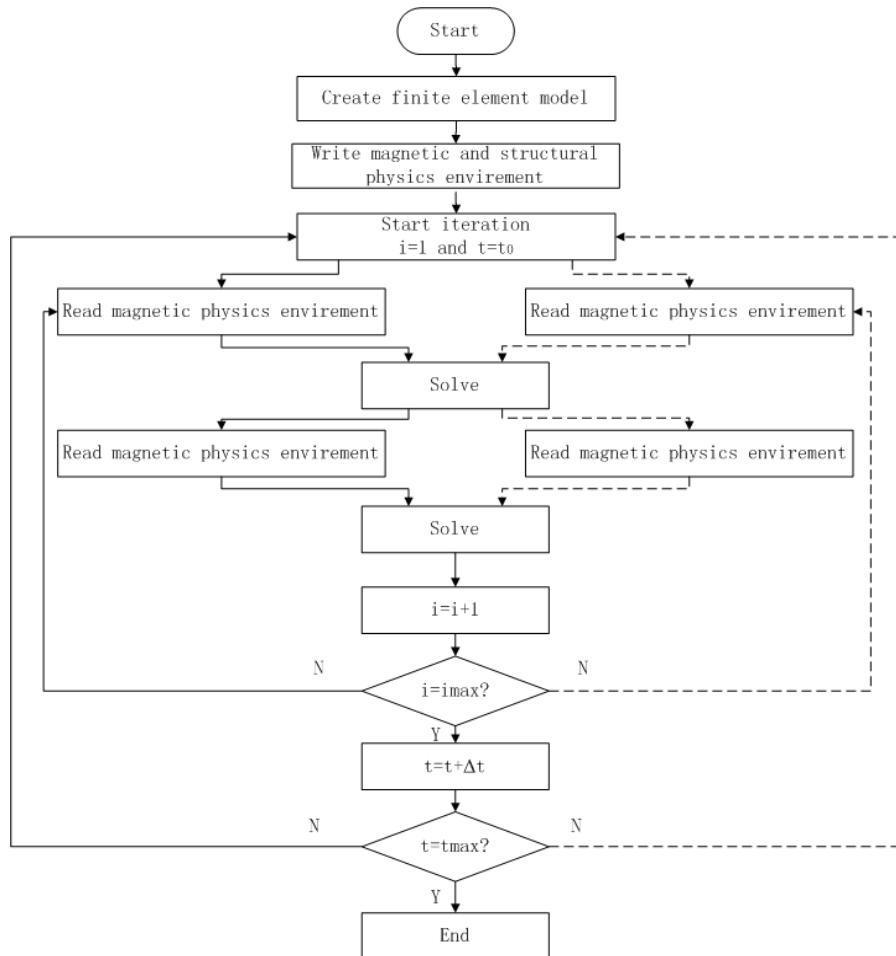


Figure 8. Scheme of magneto-mechanical coupling algorithm.

3.4. Mathematical calculation

The equivalent modulus of RVE can be calculated by equation 4-6 using the numerical results.

$$\bar{\sigma}_{ij} = \frac{1}{V} \int \sigma_{ij} d\Omega \quad (4)$$

$$\bar{\varepsilon}_{ij} = \frac{1}{V} \int \varepsilon_{ij} d\Omega \quad (5)$$

$$Modulus = \frac{\bar{\sigma}_{ij}}{\bar{\varepsilon}_{ij}} \quad (6)$$

Where, $\bar{\sigma}_{ij}$ and $\bar{\varepsilon}_{ij}$ represents the average of stress and strain in volume. V and Ω denotes the volume of the RVE and domain of integration. The superscript bar denotes the volume average of the quantity or effective quantity.

Under cyclic strain loads, energy dissipation is presented in the form of hysteresis loop and stress-strain curves were analyzed to obtain the damping properties of MRE, shown as Figure 9. Specially, damping capacity (φ) is expressed as the ratio of the dissipation energy (ΔW) during a complete cycle to the maximum storage energy (W):

$$\varphi = \frac{\Delta W}{W} \tag{7}$$

$$\Delta W = \int \bar{\sigma}_{ij} d\bar{\varepsilon}_{ij} \tag{8}$$

$$W = \int_0^{\varepsilon_0} \bar{\sigma}_{ij} d\bar{\varepsilon}_{ij} \tag{9}$$

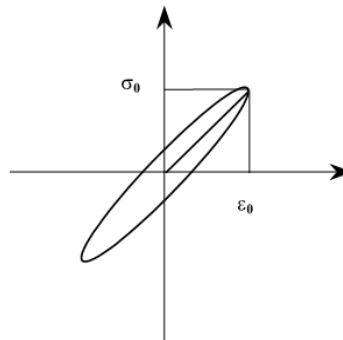


Figure 9. Stress-strain curve (hysteresis loop).

4. Results and discussion

Figure 10 and 11 shows the tensile modulus of MSR with uniform particles arrangement and chain-like particles arrangement under about 6.25% elongation, respectively. Tensile modulus shows an increasing trend with magnetic field. The results suggest that type 3 is accurate enough.

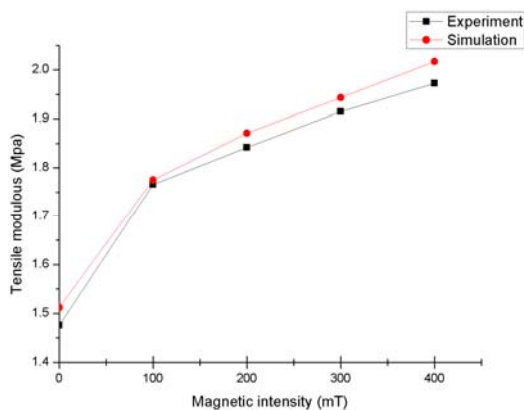


Figure 10. Tensile modulus of MSR with uniform particles arrangement.

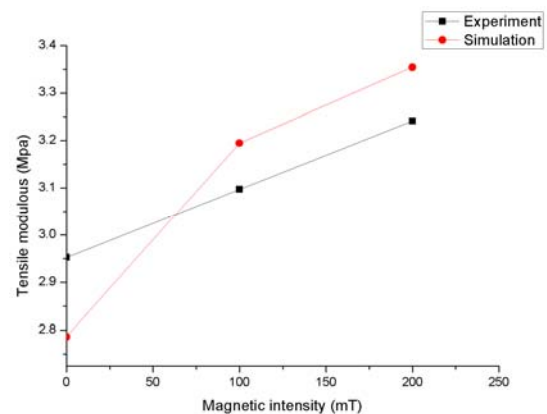


Figure 11. Tensile modulus of MSR with chain-like particles arrangement.

For dynamic experiments, sinusoidal loads with constant strain amplitudes and frequencies were applied to the MSR samples along z-axis. The real-time strain and stress signals were recorded. One strain amplitudes (2 mm) and three frequencies (1 Hz, 5 Hz, 10 Hz) as well as three magnetic fields (100 mT, 200 mT, 300 mT) were selected to study.

Figure 12 and 13 shows the field-dependence of damping capacity of the MSR under sinusoidal loads with different frequencies in experiments. In figure 13, damping capacity of MSR gets a maximum value about 1.12. Because internal defects begin to appear in MSR samples, shown as figure 14, material damping increase sharply.

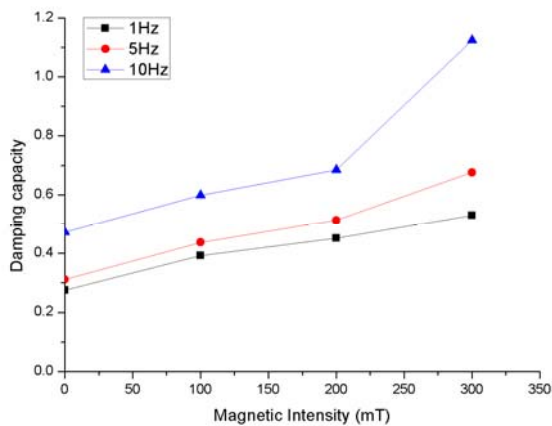


Figure 12. Damping capacity of MSR with uniform particles arrangement.

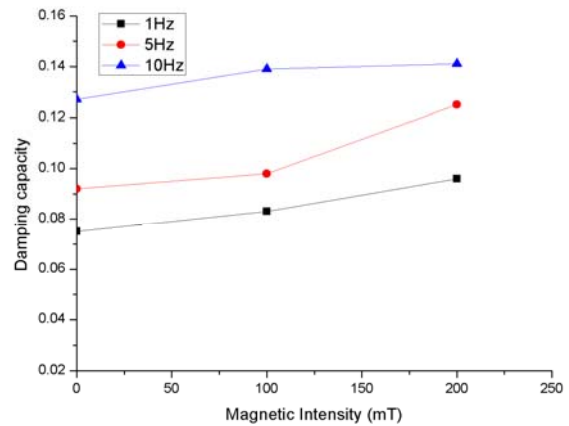


Figure 13. Damping capacity of MSR with chain-like particles arrangement.



(a) Uniform particles arrangement



(b) Chain-like particles arrangement

Figure 14. MSR with internal defects.

The shape of defects domain is similar to cylinder, which mainly locates between adjacent particles within the chain, shown as figure 15(a) and (b). These defects indicate that stress between particles is higher than other place, shown as figure 16. They will influence damping capacity.

The defects will help to explore the energy dissipation mechanisms. In figure 12 and 13, the damping capacity of MRE with uniform particles arrangement is larger than that with chain-like particles. The reason is that cylindrical matrix account for more volume fraction of the former MRE. With the increasing of magnetic intensity, the stress in cylindrical matrix will increase. Moreover, high frequency will enhance the impact of inertia force of particles. Inertia force of particles will compress the matrix. These factors will exacerbate energy dissipation that occurs within MRE through atomic level interactions such as elastic stretching of atomic bonds, vacancy diffusion and dislocation motion.

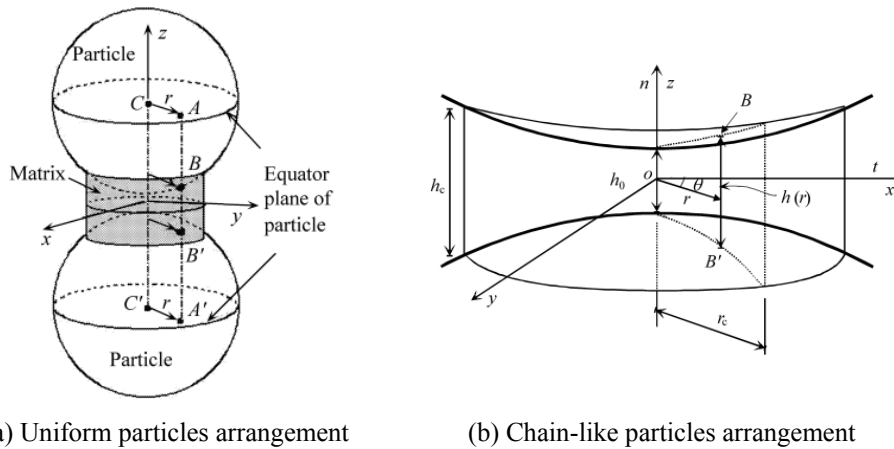


Figure 15. Adjacent particles [12].

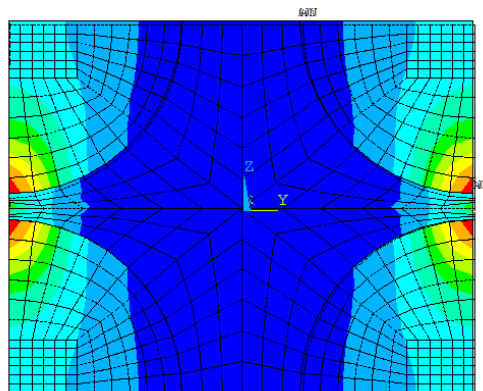


Figure 16. Distribution of stress field of MSR with chain-like particles arrangement.

5. Conclusions

A new type of MRE fabricated of iron particles with millimeter level diameter and silicone rubber is introduced. RVE including particles and matrix is built and PBC is applied. FEM based on magneto-mechanical algorithm is adopted. Both static and dynamic experiments are conducted to measure tensile modulus and damping capacity of MSR. It is concluded that the damping capacity increases with magnetic field intensity and frequency of sinusoidal loads. The cylindrical matrix between adjacent particles within the chain influence energy dissipation and are easily damaged. In the further work, small Hall probes can be installed in MSR to measure magnetic field. Moreover, photoelastic technology can be used to measure stress field of it.

Acknowledgments

This work is financially supported by the National Natural Science Foundation of China (51175016).

References

- [1] Chen L, Gong X L and Li WH 2007 *Smart Mater. Struct.* **16** 2645
- [2] Shiga T, Okada A and Kurauchi T 1995 *J. Appl. Polym. Sci.* **58** 787
- [3] Jolly M R, Carlson J D, Munoz B C and Bullions T A 1996 *J. Intel. Mater. Syst. Str.* **7** 613
- [4] Lokander M and Stenberg B 2003 *Polym. Test.* **22** 677
- [5] Bellan C and Bossis G 2002 *Int. J. Mod. Phys. B* **16** 2447
- [6] Zhou G Y 2003 *Smart Mater. Struct.* **12** 139

- [7] Ginder J M, Schlotter W F and Nichols M E 2001 *Proc. of SPIE Smart Structures and Materials 2001: Damping and Isolation* 4331 103
- [8] Demchuk S A and Kuzmin V A 2002 *J. Eng. Phys. Thermophys.* **75** 396
- [9] Shen Y and Dai H 2004 *Smart Mater. Struct.* **13** 1
- [10] Ginder J M, Nichols M E, Elie E D and Clark S M 2000 *Proc. of SPIE Smart Structures and Materials 2000: Smart Structures and Integrated Systems* **3985** 418
- [11] L.C. Davis L C 1999 *J. Appl. Phys.* **85** 3348